

# Climatology of Extreme Upper Atmospheric Heating Events

D. J. Knipp<sup>1</sup>, T. Welliver<sup>1</sup>, M.G. McHarg<sup>1</sup>, F. K. Chun<sup>1</sup>, W. K. Tobiska<sup>2</sup> and D. Evans<sup>3</sup>

<sup>1</sup>*Department of Physics, US Air Force Academy, CO, 80840, USA,*

<sup>2</sup>*Space Environment Technologies, Los Angeles, CA, USA*

<sup>3</sup>*D. Evans, Space Environment Center, NOAA, Boulder, CO, USA*

## ABSTRACT

We use a trio of empirical models to estimate the relative contributions of solar extreme ultraviolet (EUV) heating, Joule heating and particle heating to the global energy budget of the earth's upper atmosphere. Daily power values are derived from the models for the three heat sources. The SOLAR2000 solar irradiance specification model provides estimates of the daily extreme EUV solar power input. Geomagnetic power comes from a combination of satellite-derived electron precipitation power and an empirical model of Joule power derived from hemispherically-integrated estimates of high-latitude heating, which we discuss in this paper. From 1975 to mid-2002 the average daily contributions were electrons: 51 GW, Joule: 95 GW and solar: 784 GW. Joule and particle heating combine to provide more than 17% of the total global upper atmospheric heating. For the top ten and one percent of heating events, contributions rise to ~20% and 25% respectively. In the top 15 heating events geomagnetic power contributed more than 50% of the total power budget. During three events the Joule power alone exceeded solar power.

## INTRODUCTION

Heating of the upper atmosphere controls the basic structure and composition of the thermosphere. Temporal and spatial variations of the heating ultimately produce temperature changes that drive local and global circulations via the pressure gradient force. Accompanying the temperature changes are density perturbations that influence strongly the dynamics of orbiting bodies in the earth's atmosphere. Accurate satellite tracking, orbital decay prediction and orbital collision avoidance depend upon proper specification of atmospheric density. This paper provides new insight into the range and variability of three key sources of atmospheric heating: solar radiation, Joule heating and heating by low energy electron deposition.

Solar extreme ultraviolet (EUV) radiation is the single largest contributor to the upper atmospheric heating budget and is typically assumed to account for about 80% of the energy. Joule heating and precipitating particle heating, which together we call geomagnetic heating, make significant contributions to the remainder of the budget. We examine these contributions in this paper. Ion drag also contributes to upper atmospheric heating; however, our current data sets do not permit us to analyze the contribution of this source.

## BACKGROUND AND METHODOLOGY

Tobiska *et al.* [2000] report on a new model of the full solar spectrum called SOLAR2000. The model is an empirical solar irradiance specification tool for characterizing solar irradiance variability across the solar spectrum. It uses the solar irradiance proxy inputs of F10.7 for coronal emission and the Magnesium II (Mg II) core to wing ratio for chromospheric emission. Thermospherically effective irradiances are modeled at 1 nm resolution between 1 and 10<sup>6</sup> nm and reported in SI units of W m<sup>-2</sup> at one Astronomical Unit. The constituent volume heating rate is reported in giga-watts (GW). Recent modifications to the SOLAR2000 model allow for height-integrated, daily estimates of the solar EUV power. In the model energy deposition is in the 150-200 km range for almost all levels of solar activity. Consistent with the variations in solar EUV output, the magnitude of heating in all altitudes above 100 km changes substantially with solar activity. Daily estimates of power can be made for the interval from 1947 to mid-2002 with the more reliable values available after 1976.

Instruments on board the NOAA TIROS and Polar-orbiting Operational Environmental Satellite (POES) continually monitor the power flux carried by the protons and electrons that produce aurora in the atmosphere.

Fuller-Rowell and Evans [1987] developed a technique that uses the power flux observations obtained during a single pass of the satellite over a polar region (which takes about 25 minutes) to estimate the total power deposited in an entire polar region by the 50 eV to 20 keV particles. Recently Hubert *et al.* [2002] showed hemispheric proton power contributions typically to be less than 10 GW. They also noted that proton power was a smaller fraction of particle power during active times. In this study we estimate only the global precipitating electron power, but we add a constant 15 GW of proton power to account for the global contribution to the power budget. We averaged the southern hemisphere passes for each day from mid-1991 to mid-2002 to create daily estimates of the electron precipitating power. Only the southern hemisphere data were used because the satellites' tracks through the southern hemisphere cut more directly through the auroral zone, thus giving a better and more consistent estimate of the auroral electron power.

Joule power is closely associated with the level of geomagnetic activity. Chun *et al.* [1999] estimated hemispheric Joule heating with a quadratic fit to the Polar Cap (PC) Index, which is a proxy for the electric field imposed on the polar ionosphere by the solar wind [Troshichev *et al.*, 1988]. They assembled a set of 12,000 hemispherically integrated Joule heating values derived from the Assimilative Mapping of Ionospheric Electrodynamics (AMIE) mapping procedure [Richmond and Kamide, 1988] as a statistical ensemble for binning Joule power against geomagnetic activity. They noted the model underestimated Joule heating during strong storms. We have addressed that concern by including another fit parameter to improve the power estimates during storm time. Using a series of multiple linear regression fits, we determined that the Joule heating could be better parameterized using the Polar Cap (PC) index and the Disturbance Storm Time (Dst) index. The Dst index can be thought of as a proxy for the electrical interaction of the nightside magnetosphere and ionosphere. We chose the regression parameters, PC and Dst, based on their: 1) association with geomagnetic activity; 2) hourly cadence and, 3) relatively long-term, uninterrupted availability. As shown in Table 1, Joule power is dependent on quadratic fits to both PC and Dst. The variations in seasonal coefficients are in part due to seasonal changes in conductivity. We applied the seasonal coefficients to derive the Joule power presented in this paper.

Table 1. Fit Coefficients for Joule Power

Fit Season	Months	Fit Using Absolute Values of PC and Dst	R <sup>2</sup>
Annual	Jan-Dec	$JH(GW)=24.89*PC + 3.41*PC^2 + .41*Dst + .0015*Dst^2$	0.76
Winter	21 Oct-20 Feb	$JH(GW)=13.36*PC + 5.08*PC^2 + .47*Dst + .0011*Dst^2$	0.84
Summer	21Apr-20 Aug	$JH(GW)=29.27*PC + 8.18*PC^2 -.04*Dst + .0126*Dst^2$	0.78
Equinox	21Feb-20Apr, 21Aug-20Oct	$JH(GW)=29.14*PC + 2.54*PC^2 +.21*Dst + .0023*Dst^2$	0.74

The AMIE values which provide the foundation for the fits are calculated over a northern hemisphere grid (typically 2.0° in magnetic latitude,  $\Lambda$ , and 15° in longitude) using the product of the height-integrated Pedersen conductance and the square of the electric field value in each grid box. Integration over the grid from 40°  $\Lambda$  to the magnetic pole produces hemispherically-integrated values of Joule power. A comparison of AMIE derived Joule heating and the model empirical results are shown for the strong equinox storm of March 20-21, 1990 in Figure 1. This figure and the correlation coefficients in Table 1 indicate that the PC-Dst combination can provide a good proxy measure of simple, large-scale Joule heating on a global scale. We do not yet account for small-scale variability of the electric field, which may add considerably to the Joule heating tally during very quiet and very disturbed times. Neither do we account for neutral wind effects that contribute to the power budget when the ion flows are significantly different from neutral wind motions. Thus, our geomagnetic power estimates are probably conservative. These shortcomings aside, we note that the geomagnetic power values provided here are consistent with an overall 17% geomagnetic contribution to upper atmospheric heating.

## RESULTS

Using the models described above, we calculated the power input to the upper atmosphere. Table 2 summarizes the average power estimates and standard deviations over all of the solar cycles and over the solar minimum and solar maximum years. The bottom two rows of Table 2 present the statistics for the top 10% and the top 1% of the heating events. Figure 2 shows the daily power input to the upper atmosphere derived from the SOLAR2000

model, the precipitating particles and our estimated Joule power. From bottom to top the curves are: particle precipitation power, Joule power, solar EUV power and total power.

Table 2. Summary of Average Power and Variability

Power Category:		Proton (GW)	Electron (GW)	Joule (GW)	Solar (GW)	Total (GW)
Solar Min: 75-77, 83-87, 93-97	Avg St Dev	15 (2%)	37 (5%) 8	76 (11%) 62	550 98	678 134
Solar Max: 78-82, 88-92, 98-02	Avg St Dev	15 (1%)	54 (5%) 56	111 (9%) 111	995 242	1175 281
Solar Cycles 21-23	Avg St Dev	15 (2%)	51 (5%) 33	94 (10%) 92	784 291	944 330
Top 10% of heating events	Avg St Dev	15 (1%)	77 (5%) 49	202 (13%) 197	1308 1434	1602 195
Top 1% of heating events	Avg St Dev	15 (1%)	98 (5%) 49	363 (19%) 305	1357 135	1833 338

The daily geomagnetic power delivered to both auroral zones is shown in the bottom curves of Figure 2. For simplicity this estimate is made by doubling the northern hemisphere value of Joule power and the southern hemisphere value of electron precipitation power. In the future we hope to include better independent hemispheric estimates. The darker bottom curve shows the precipitating particle power from mid-1991 to mid-2002 (including 15 GW for proton power). These particles contribute only a small fraction (7%) of the total power to the upper atmosphere. On average the precipitating electrons produce 51 GW of power with a standard deviation of 33 GW. In order to make a reasonable comparison of total power for the interval 1975 to mid-1991 when there were significant gaps in particle power data, we included the average value of the POES precipitating power, 26.1 GW, for the solar maximum years (1991-1992 and 1998-2002) and the power, 24.7 GW, for solar minimum years (1993-1997) as an estimate of the electron power. They are shown as the nearly straight line in Figure 2. The lighter bottom curve shows Joule power for the interval 1975 to mid-2002. The daily Joule power ranges from 7 GW in 1997 to 2035 GW in 1982. Across the three solar cycles the daily Joule power input to the upper atmosphere is roughly 95 GW. The standard deviation of the daily Joule power is 92 GW. Although the most extreme values of Joule heating tend to occur during solar maximum years, significant Joule heating events with daily power in excess of 500 GW occur even during solar minimum years. The extreme Joule power events are typically accompanied by NOAA POES estimates of particle power in excess of 200 GW.

Daily solar EUV power is the lighter upper curve. The range of solar power extends from a low of 459 GW in 1995 to a maximum of 1692 GW in 1989. The average daily solar power input to the upper atmosphere is 784 GW with a standard deviation of 291 GW. The largest values of solar power occurred in the early years of solar cycles 21 and 22. Solar cycle 23 differed from the previous cycles in that the peak power was delivered toward the end of the solar maximum phase.

The top dark curve in Figure 2 shows the temporal variations of the total power. The minimum value of total power, 525 GW, occurred in 1977, while the maximum value of 3376 GW occurred in 1982. The dates of the top 10 total daily heating events (of ~10,000 days) are specifically labeled in Figure 1. Among these dates are the notorious March 1989 and July 2000 storms. For the top 10% of all daily heating events Joule heating was the most variable contributor. The top 1% of all heating events occurred exclusively during solar maximum years. Of these events more than half had substantial contributions from Joule power (Joule power contributed ~ 20% of the daily heat budget). For the 15 most extreme events (listed in Table 3) geomagnetic heating constituted approximately 50% of the energy budget. These extraordinary events are defined roughly by the following conditions: Total Joule power greater than 600 GW and geomagnetic power great than or equal to 50% of total power. During the three most powerful events Joule power alone exceeded the solar EUV power. From these data it is apparent that Joule power is an extremely variable component of the upper atmospheric heat budget and is a major player in the largest storms.

Table 3. Top 15 Daily Power Events

Yr	Rank	Month/ Day	Electron Pwr (GW)	Joule Pwr (GW)	Solar Pwr (GW)	Total Pwr (GW)	% Geo- magnetic Pwr
1982	1	7/14	52*	2035	1289	3376	62
1989	3	3/13	52*	1576	1270	2899	56
1989	9	10/21	52*	1059	1250	2361	47
1991	13	3/24	52*	930	1282	2265	43
1991	4	6/5	244	1082	1321	2647	50
1991	12	6/11	166	811	1348	2325	42
1991	10	7/9	171	867	1321	2359	44
1991	15	7/13	176	817	1234	2227	45
1992	6	5/10	224	1484	828	2536	67
2000	11	7/15	77	1083	1186	2347	49
2000	7	7/16	105	1144	1225	2474	50
2000	14	8/12	97	1040	1116	2252	50
2001	5	3/31	285	878	1474	2637	44
2001	2	11/6	231	1518	1301	3050	57
2001	8	11/24	205	1027	1165	2397	51
		Avg:	180	1157	1241	2543	50

\* Value not known due to lack of coverage or detector deterioration, average solar cycle value used.

## SUMMARY

Using a trio of empirical models we have quantified the relative roles of particle power, Joule power and solar EUV power. Although we have not included ion drag effects and power contributions from small scale electric field variability, we still gain a strong sense of the role of geomagnetic power variability: On average geomagnetic power contributes just over 15% of the total power value, but over one third of the power variability. In the top 10% of geomagnetic heating events, geomagnetic power provides ~ 20% of the total heating and is the dominant contributor to the variability. For the top 15 events geomagnetic power was more than 50% of the total power.

We recognize that temporal variations of power values alone are not sufficient to specify the atmospheric density perturbations likely to be encountered by bodies orbiting in the earth's atmosphere. Nonetheless this exercise in power estimation represents a significant step in understanding the pivotal role that geomagnetic heating can play in satellite drag, orbital perturbations and other dynamical effects in the upper atmosphere. We conclude that geomagnetic heating can be a source of significant error in satellite orbit calculations even during solar minimum.

## Acknowledgements

DJK, MGM and FCK were supported by National Science Foundation Grant 0077536.

The Polar Cap data were provided by the Danish Meteorological Institute, The Dst Index was provided by World Data Center 2, Kyoto, Japan and the NASA National Space Science Data Center. We wish to thank Dr Barbara Emery who helped process the data for Figure 1.

## References

- Chun, F. K., D. J. Knipp, M. G. McHarg, G. Lu, B. A. Emery, S. Vennerstrøm, and O. A. Troshichev, Polar cap index as a proxy for hemispheric Joule heating, *Geophys. Res. Lett.*, 26 (8), 1101-1104, 1999.
- Fuller-Rowell, T. J., and D. S. Evans, Height-integrated Pedersen and Hall conductivity patterns inferred from the TIROS-NOAA satellite data, *J. Geophys. Res.*, 92, 7606, 1987
- Hubert, B., J. C. Gerard, S. D. S. Evans, et al, Total electron and proton energy input during auroral substorms: Remote sensing with IMAGE-FUV, *J. Geophys. Res.*, 107, 2002
- Richmond, A.D. and Y. Kamide, Mapping electrodynamic features of the high latitude ionosphere from localized observations: Technique. *J. Geophys. Res.*, 93, 5741, 1988
- Tobiska, W. K., T. Woods, F. Eparvier, et al., The SOALR2000 empirical solar irradiance model and forecast tool, *J. Atmos. and Solar Terr. Phy.*, 62, 1233, 2000
- Troshichev, O. A., V. G. Andersen, S. Vennerstrom and E. Friis-Christensen, Magnetic activity in the polar cap: A new index, *Planet. Space Sci.*, 36, 1095, 1988

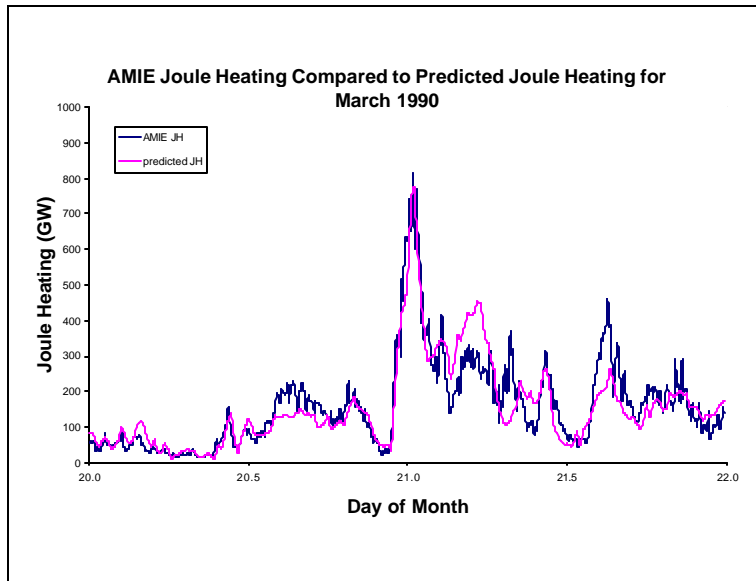


Fig. 1. Joule power derived from the AMIE procedure using hundreds of data points compared to the proxy Joule heating values derived from the least squares fit to the ground magnetic indices shown in Table 1.

### Daily Average Power Values for Solar Cycles 21-23

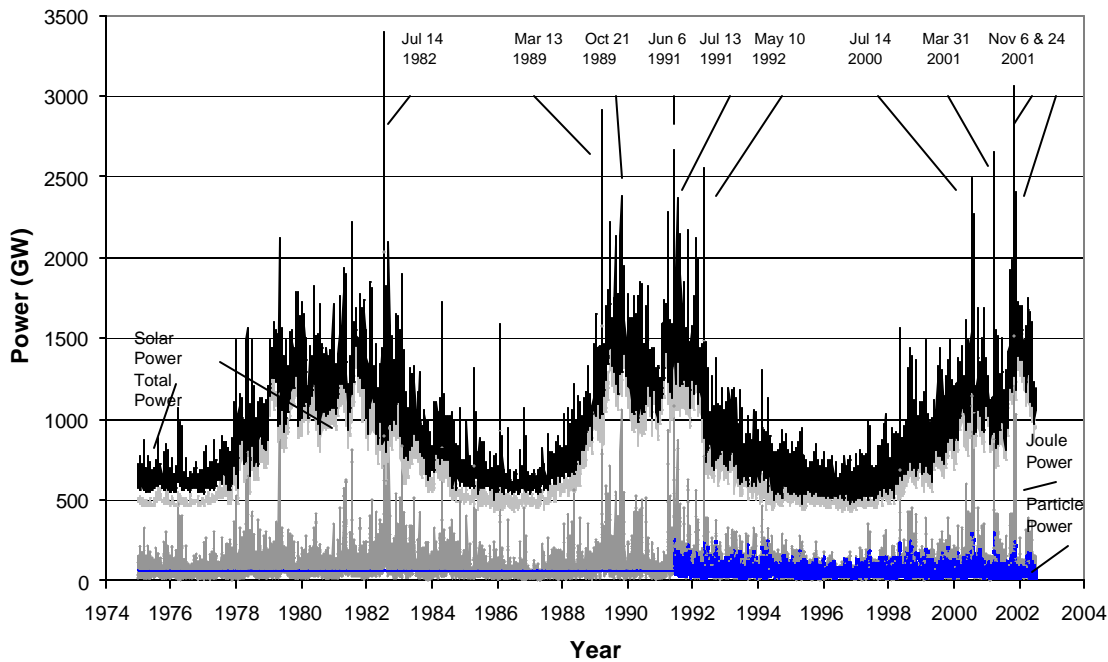


Fig. 2. Estimates of the precipitating particle power, Joule power, solar power and total power from 1975 to mid-2002. An average of the average of most recent solar cycle's precipitating particle power is used for 1975 to mid 1991.

### Joule Heating Vs Total Heating

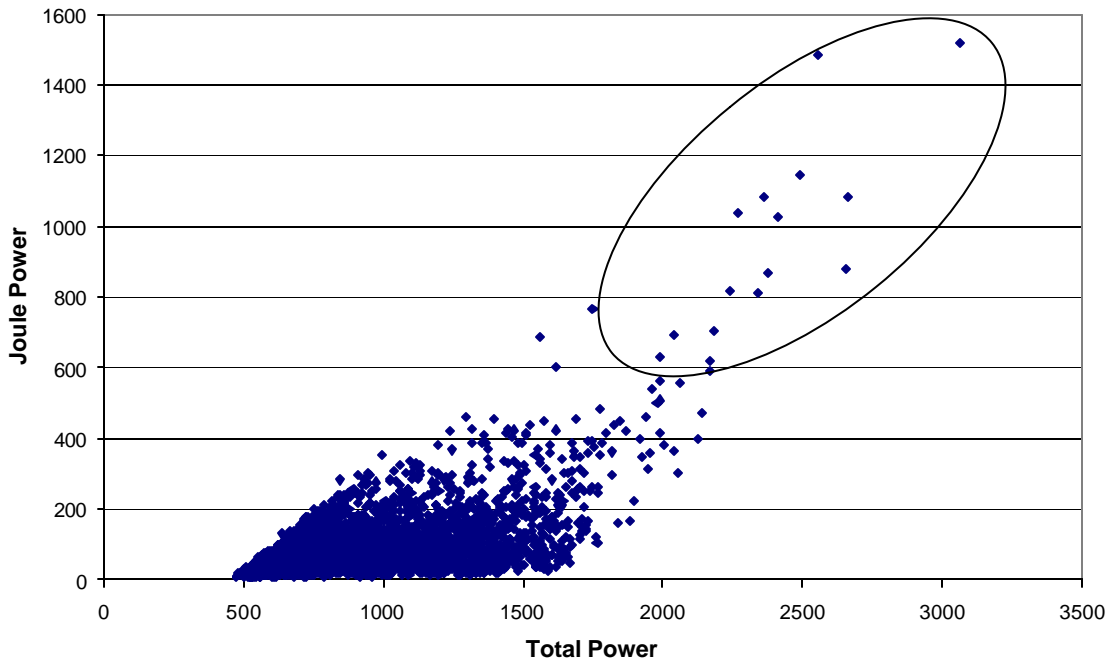


Figure 3. Scatter plot of global Joule versus total heating. The points within the oval constitute the 15 most extreme heating events between 1975 and mid-2002. Power values for these events are presented in Table 3.